Soft Matter

Cite this: *Soft Matter*, 2011, **7**, 10025

www.rsc.org/softmatter

PAPER

Facile photopatterning of polyfluorene for patterned neuronal networks†

Nam Seob Baek,[a] Yong Hee Kim,[a] Young Hwan Han,[a] Bong Joon Lee,[a] Tae-Dong Kim,[b] Sin-Tae Kim,[b] Young-Seok Choi,[a] Gook Hwa Kim,[a] Myung-Ae Chung[a] and Sang-Don Jung*[a]

Received 15th May 2011, Accepted 28th July 2011
DOI: 10.1039/c1sm05894k

In this paper, we demonstrated a facile photopatterning method that uses photocrosslinkable polyfluorene to fabricate micro-sized photopatterns on transparent indium tin oxide substrate for neuronal patterning. The modified poly(ethyleneimine) (m-PEI) with trimethoxysilane moiety was chemically attached to the hydroxyl group-terminated ITO surface and then the photopatternable polyfluorene derivative was spin coated as a cell-repellent layer onto the m-PEI-coated surface. The well-defined micropatterns were easily created over an entire surface by photocrosslinking of bromoalkyl-substituted polyfluorene (Br-PF) *via* the radical coupling reaction of a C–Br bond under UV irradiation without an initiator. UV-Vis absorbance, photoluminescence, ATR-FTIR and X-ray photoelectron spectroscopy were used to confirm the photocrosslinking process and the surface composition before and after the photocrosslinking of polyfluorene. The pairing of adhesive m-PEI and repulsive Br-PF effectively guided the neurite outgrowth and controlled neurite extension from individual neurons to the pre-patterned direction with excellent pattern fidelity. Guided neuronal cells were maintained for at least 25 days *in vitro* without any detachment of neuronal cells during cell culture. A photopatternable polyfluorene derivative in combination with cell-adhesive m-PEI is proved to be an effective way to modify the electrode surface to achieve single cell level neuronal networks.

Introduction

Artificial neuronal networks *in vitro* are a useful tool in studying brain diseases and examining the communication between neuronal cells and electronic devices. In order to achieve the desired neuronal network *in vitro*, the specific ability of cell-adhesive molecules (CAM) to create finely patterned substrates, *via* some appropriate surface modifications, is required. The appropriate surface modification that can promote cellular adhesion and growth in bio-active devices plays a critical role in the development of multi-electrode arrays (MEAs)[1,2] and neurochips[3,4] or biosensors.[5] Controlling the interface between patterned electrodes coated with CAM and neurons plays an important role in the interpretation of the cellular behavior of neuronal networks in MEAs[6] and can significantly improve the device performance.[7] Conventionally, the patterned substrate for a neuronal network consists of the cell-adhesive region coated with a positively charged polymer[8] and the cell-repellent region.[9] Up to now many researchers have fabricated the patterns of CAM by means of photolithography,[10] soft lithography techniques like micro-contact printing,[11,12] or deep UV lithography techniques[13] in combination with surface chemistry to chemically immobilize CAM on the substrate.[14] Although the soft lithography protocol is a well-established method and is commercially used to fabricate pre-patterned surfaces, expensive instruments and multistep processes were necessary and it is hard to produce narrow micropatterns (<10 μm) for a single-cell-based neuronal network.

In our previous work, we fabricated micron-scale patterns from the photodegradation of biocompatible modified-poly (ethyleneimine) (m-PEI) that was chemically bound to the surface of indium tin oxide (ITO).[15] The photopatterned m-PEI layer facilitated the uptake of neuronal cells in the designed pattern and was capable of controlling the neurite outgrowth and extension along the patterned direction. However, it took a relatively long exposure time in fabricating the desired patterns *via* photodegradation of m-PEI by deep UV (254 nm) irradiation. Even though we can save the exposure time by adopting a strong intensity UV source, it costs too much. The other drawback of the fabrication of patterns from the photodegradation of m-PEI is that it is hardly possible to get neuronal networks free from neurons and their connections presenting in the space areas in the grid-space type pattern. This drawback results from the exposure of hydrophilic ITO or silicon oxide surface after developing of photodegraded m-PEI. Although neuronal cells are not spontaneously adhered to the surface of

[a]*IT Convergence Technology Research Laboratory, Electronics and Telecommunications Research Institute, Daejeon, 305-700, Republic of Korea. E-mail: jungpol@etri.re.kr; Fax: +82 42 860 6564; Tel: +82 42 860 5557*
[b]*Department of Advanced Materials, Hannam University, Daejeon, 305-811, Republic of Korea*
† Electronic supplementary information (ESI) available: Fig. S1, S2, S3, S4, S5 and S6. See DOI: 10.1039/c1sm05894k

ITO and silicon oxide they do not completely lose the chance because of the biocompatible and hydrophilic nature of ITO and silicon oxide.

In order to save fabrication time and get neuronal patterns devoid of neurons presenting in the space area we adopted a photocrosslinking system and a hydrophobic surface instead of the time-consuming photodegradation and a hydrophilic surface. For this we have selected polyfluorene (PF) as the photocrosslinking system. Owing to the fluorene group, it is hydrophobic so that it can repel neuronal cells, resulting in the confinement of neuronal cells to the neuronal cell-adhesive region. Biocompatible and water-soluble polyfluorene derivatives have been used as a probe for DNA sequence detection[16] and a singlet oxygen generator.[17] Small features sized less than 1 μm are routinely obtained from photocrosslinkable polymers.[18,19] However, many photocrosslinkable polymers need a photo initiator, like diphenyiodonium hexafluoroarsenate, for initiation of photocrosslinking. Because of the potential toxicity the use of a conventional photo initiator is not a proper solution for biomedical applications. To solve this we have introduced bromoalkyl groups into PF. The bromoalkyl-substituted polymers can be sufficiently crosslinked *via* a radical coupling reaction initiated by the cleavage of the C–Br bond in the absence of a photo initiator.[20] Furthermore, the biocompatible crosslinking of Br-PF occurs using UV light, but not thermal treatment. Therefore, the nontoxicity and low temperature processing for the fabrication of patterned substrates are suitable for bio applications.

For these reasons, we have introduced Br-PF layer onto the m-PEI layer followed by area-selective photoexposure. The photoexposed Br-PF is crosslinked and acts as a neuronal cell repellent, whereas the intact Br-PF is stripped and the naked positively charged m-PEI attracts negatively charged neuronal cells. Here, we describe the facile photopatterning characteristics of photocrosslinkable Br-PF and neuronal cell-repellent performance in detail.

Results and discussion

The synthesis of Br-PF is shown in Scheme 1. 2,7-dibromo-9,9′-bis(6′′-bromohexyl)fluorene and 2,2′-(9,9-dioctyl-9*H*-fluorene-2,7-diyl)bis(4,4,5,5-tetramethyl-1,3,2- dioxaborolane) were prepared according to the methods described in the literature.[21,22] The polyfluorene derivative (Br-PF) was prepared *via* Suzuki cross coupling reaction catalyzed by $Pd(PPh_3)_4$ in toluene to give photopatternable polymer as a yellowish solid. The chemical structures involved in this study were identified by FT-IR, ^{1}H-NMR, GPC, UV-Vis absorption and fluorescence spectroscopy. ^{1}H-NMR spectra of materials used in this paper are presented in Fig. S1.†

In the NMR spectrum, the observed δ values for bromomethyl protons (–C$\underline{H}_2$Br, 2H) and for dioxaborolane (–C$\underline{H}_3$, 12H) in monomers are 3.3 ppm and 1.39 ppm, respectively. After coupling of the dibromo-functionlized monomer (M1) with dioxoborolan-functionlized monomer (M2), yielding the photocrosslinkable polyfluorene, the terminal dioxoborolan proton had clearly disappeared in the ^{1}H-NMR. The thermal stability of the resulting polymer was evaluated by differential scanning calorimetry (DSC) and thermogravimetric analysis (TGA) measurements at a heating rate of 10 °C min^{-1}. The T_g of synthesized PF is 72 °C and its degradation onset is ~260 °C. The first decomposed region is attributed to the degradation of long alkyl chains and the second one is due to the decomposition of the polymer backbone. The synthesized Br-PF seems to be thermally stable and is a suitable material to fabricate photopatterned substrate as a cell-repellent layer.

Scheme 2 shows a schematic diagram of the photopatterning procedure for the fabrication of micro-sized patterns. Details of photopatterning procedures and patterned neuronal cell culture are described as following. The ITO substrate treated with a mixture of NH_3 : H_2O_2 : H_2O (1 : 4 : 20 v/v) solution at 70 °C for 1 h was immersed in a 2% m-PEI solution under N_2 atmosphere overnight. The positively charged m-PEI are covalently linked to the pre-treated ITO surface *via* sol–gel process.[23] 1 wt% Br-PF solution was then spin-coated (1500 rpm for 30 s) on the m-PEI surface, resulting in the formation of a pinhole free thin film. In order to get the designed micropattern the Br-PF coated substrate was placed in a mask aligner equipped with a constant power (P_{325nm} = ~60 mW cm^{-2}) supply and then exposed for 360 s without a photo initiator. After UV exposure, the substrate was rinsed with $CHCl_3$ solution for 5 min followed by washing with acetone, resulting in a specific micropattern with a thickness of *ca.* 26 ± 1 nm measured by alpha step profilometer for neuronal pattering.

To confirm the photocrosslinking of polyfluorene, we monitored the changes in ATR-FTIR, UV-Vis absorption and emission spectra with respect to the exposure time. UV-Vis absorption and photoluminescence (PL) spectra of polyfluorene bearing photocrosslinkable substituents are shown in Fig. 1. The absorbance of the uncrosslinked Br-PF film showed a maximum at 383 nm, similar to that of a water-soluble polyfluorene derivative[16,24] and the fluorescence maximum appeared at a wavelength of 441 nm with well-resolved structures when excited at 370 nm. After photoexposure, there are almost no changes in UV-vis absorption behavior. However, the emission

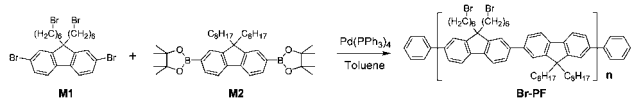

Scheme 1 The synthesis of photocrosslinkable polyfluorene derivative.

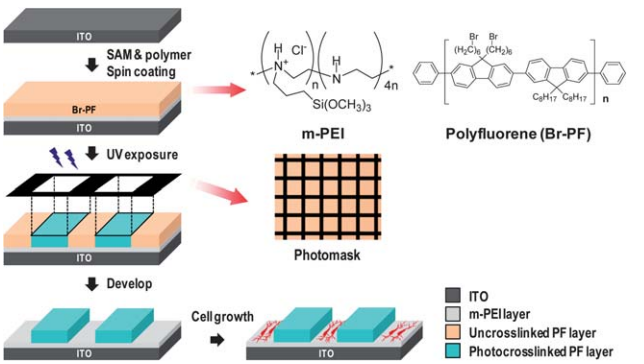

Scheme 2 A diagram of the photopatterning processes for patterned neuronal cell growth.

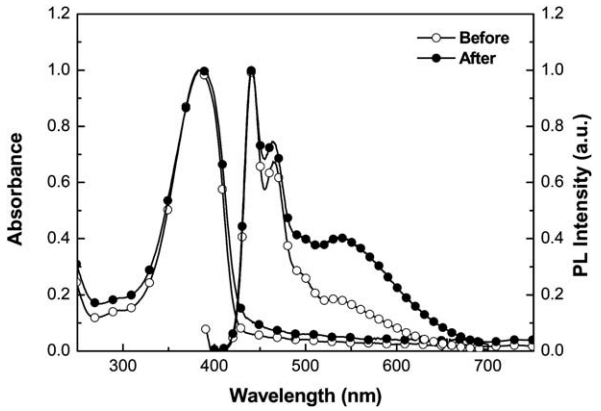

Fig. 1 Normalized UV-Vis absorption and photoluminescence spectra (λ_{ex} = 370 nm) of Br-PF film before and after photoexposure (360 s).

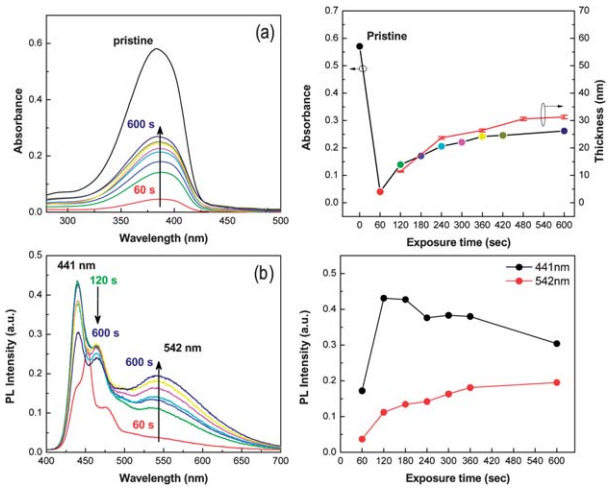

Fig. 2 Changes in UV-Vis absorption and PL intensities of crosslinked Br-PF film with respect to exposure time (measured after rinse with $CHCl_3$).

spectrum of the photoexposed Br-PF film differs from that of the unexposed film in that the intensity of green emission peak increases with increasing exposure time. The rather broad green emission has been reported for many conjugated polymers and attributed to the formation of excimers and/or aggreagates.[25] The photocrosslinking should reduce the intermolecular distances between emissive chromophores and thus can increase the probability to form excimers and/or aggregates through intermolecular interaction. The degree of aggregation of polyfluorene chains is known to be strongly affected by the molecular weight of the polymer,[26] the type of side-chain,[27] and the end group of the polymer chain.[28] Even though defective ketones generated during the thermal annealing in air can produce green emissions,[29,30] the generation of ketones can be avoided by performing the baking and photoexposure under nitrogen atmosphere.[30] For example, we could not find any significant evidence for the oxidation of the substituent hydrogens in the 9-position of the fluorene unit from the ATR-FTIR spectrum before and after the photocrosslinking process under nitrogen environment (Fig. S2 in the ESI†). In FT-IR, characteristic bands of m-PEI coated on ITO substrate, corresponding to N–H stretching and scissoring (broad 3300 cm^{-1} and 1673 cm^{-1}), alkyl C–H (2947–2830 cm^{-1}), and Si–O–Si (1132–1050 cm^{-1}) stretching were observed.[15] In the crosslinked Br-PF film, the vibrational peaks at 2939 and 2861 cm^{-1} for the C–H stretch vibrations of the aliphatic side-chain in the fluorene unit and 1612 cm^{-1} for the aromatic C=C stretch vibration were observed before and after photocrosslinking.

In order to see the effect of exposure time on the formation of patterns and to determine the proper exposure time, Br-PF was spin-coated onto the quartz plate and exposed for 30 s to 600 s under nitrogen atmosphere (Fig. S3 in the ESI†). The exposure was performed with and without a Cr photomask. After exposed samples were rinsed with chloroform to strip the uncrosslinked fraction of Br-P, thickness measurements were done with the samples exposed with the Cr photomask. As shown in Fig. 2(a) the absorbance and the photocrosslinked film thickness increased with increasing exposure time, indicating that the photocrosslinking progresses gradually. The increase in intensity of the broad emission band with increasing exposure time, shown in Fig. 2(b), can be explained in terms of the formation of excimers and/or aggregates with respect to the exposure time and confirms the progress of photocrosslinking. Since the exposure time dependence of absorbance, broad green emission and the pattern thickness are closely linked with each other, we can predict the pattern thickness from absorbance or emission spectra. For example, we can get a pattern with the desired thickness through the *in situ* monitoring of the broad green emission intensity while photocrosslinking.

Notwithstanding its simplicity, contact angle measurement enables us to qualitatively and quickly check the many processes involved in the surface modification. Table 1 summarizes the contact angles of bare ITO, pre-treated ITO, m-PEI layer and the photopatternable polyfluorene layer before and after photoexposure (Fig. S5 in the ESI†). The contact angle of bare ITO decreased from 58 ± 4° to 35 ± 2° by means of chemical treatment, resulting in an increase of oxygen groups on the ITO surface. The pre-treated ITO substrate was immersed in 2% m-PEI solution. The contact angle of the m-PEI layer was slightly increased. After spin coating of the Br-PF solution onto a m-PEI layer, contact angle for unexposed Br-PF film is 98 ± 2°, which closely matched the linear alkyl-substituted polyfluorene spun casted on quartz or silicon substrate (100–103°).[31] Once photocrosslinked, the contact angle of exposed Br-PF film did not significantly change after washing with $CHCl_3$ solution. Owing to its hydrophobic nature, the patterned Br-PF film can act as a cell-repellent layer.

To check the chemical compositions of the film, each layer was evaluated by XPS measurement. XPS spectra of the m-PEI layer and the Br-PF layer were depicted in Fig. 3. On the chemical binding of m-PEI to ITO surface, the binding energies of C 1s, N 1s and Si 2p atoms in the m-PEI moiety were observed at 284.5 eV (C–C/C–H) and 286.4 eV (C–N), 398.9 eV and 101.9 eV, respectively.[15] To quantitatively analyze the chemical compositions and demonstrate the cleavage of C–Br bond during the photocrosslinking process, 1wt% Br-PF solution was spin-coated onto the quartz substrate and anlyzed by XPS. The photocrosslinking process was monitored by the decrease in the intensity of Br 3d peak under the same experimental conditions (Fig. 3). In unexposed Br-PF film, peaks of 284.5 eV for C 1s,

Table 1 Contact angles of bare ITO, pre-treated ITO, m-PEI layer and Br-PF layers before and after photoexposure

Substrate	Bare ITO	Pre-treated ITO[a]	m-PEI[b]	Unexposed Br-PF[c]	Exposed Br-PF[d]
Contact angle (°)	58 ± 4	35 ± 2	44 ± 1	98 ± 2	93 ± 2

[a] chemical treatment. [b] surface modification by sol–gel reaction. [c] spin-coated film. [d] after photocrosslinking.

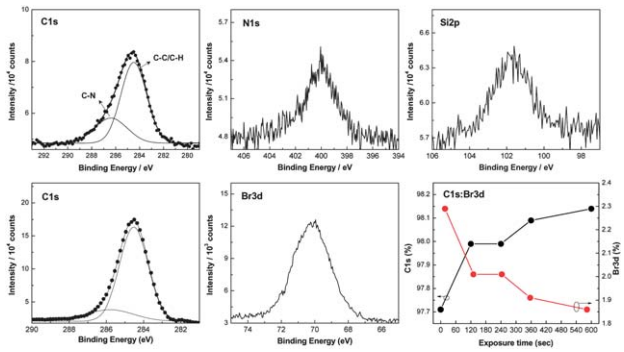

Fig. 3 (top) XPS spectra of m-PEI layer on ITO substrate and (bottom) Br-PF layer cast on quartz substrate (relative ratio of C 1s to Br 3d species as a function of exposure time).

532.2 eV for O 1s and 101.8 eV for Si 2p were observed. Also, characteristic peaks at 71 eV for Br 3d, 185 eV and 192 eV for Br 3p and 259 eV for Br 3s were detected, corresponding to carbon-bound bromine in the Br-PF (Wide-scan XPS spectra in Fig. S6†).[32]

Analysis of the C 1s : Br 3d ratio as a function of exposure time was carried out. Apparently, the Br 3d intensity becomes gradually decreased with increasing exposure time from pristine film (2.29%) to 600 s dose (1.86%). Additionally, the intensity of the C 1s component is relatively increased from 0 s (97.71%) to 600 s dose (98.14%), suggesting that photocrosslinking of Br-PF film occurs due to the radical coupling reaction initiated by the cleavage of the C–Br bond. These results are consistent with the degrees of crosslinking of the Br-PF film. As a result, it is likely that photopatternable Br-PF is easily formed into a well-defined lattice with a relatively short exposure time. We have arbitrarily fixed 360 s as a proper exposure time and fabricated patterns with various features to see the photopatterning fidelity of Br-PF.

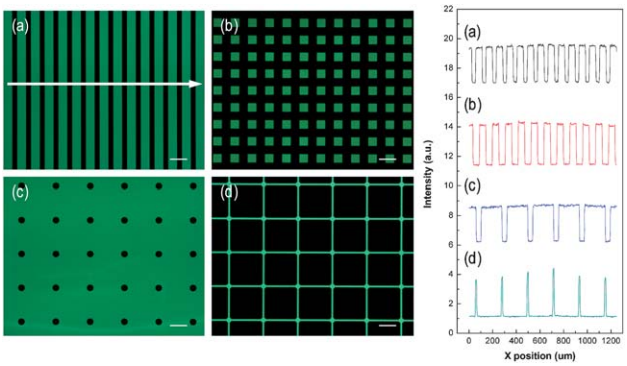

Fig. 4 Fluorescence images and intensity profiles of photocrosslinked Br-PF pattern on quartz substrate. All scale bars are 100 μm.

Fig. 4 shows a fluorescence image of photocrosslinked patterns and intensity profiles of the patterns. In particular, the pattern of Fig. 4(d) is designed to fit to a conventional 64-channel MEA feature with 10 μm line width and 200 μm spacing. Even though, due to lack of a photomask, we obtained patterns with the minimum feature size of 4 μm, this result does not limit pattern fidelity of Br-PF to 4 μm and it seems possible to get even submicron patterns. In patterned neuronal growth, single neuron level connections are required so that a pattern line width of 6–10 μm is a reasonable window considering the size of a single cell, around 10 μm in diameter. This consideration leads to the fact that the photocrosslinkable Br-PF, in combination with its biocompatibility,[17] has sufficient pattern resolution suitable for use in patterned neuronal growth.

To verify the neuronal cell confining ability of hydrophobic Br-PF, we have cultured hippocampal neuronal cells on the grid-type micropattern, (d) in Fig. 5. The outmost surface of the grid and the space is consisted of m-PEI and Br-PF, respectively. A feature spacing of 200 μm was maintained for potential application of this method to commercially available MEAs. Compared to straight lanes, the grid-space type micropattern provides substrates for long-term cell growth so that neuronal cells were maintained for longer than 25 days *in vitro* (DIV).

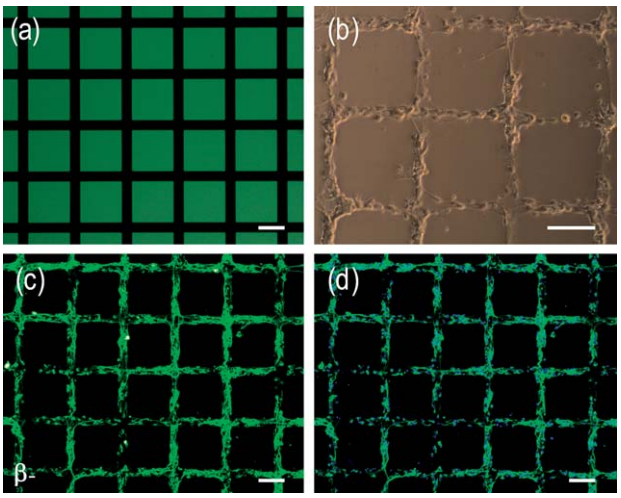

Fig. 5 (a) Fluorescence micrographs of the grid micropattern (360 s UV exposed and rinsed with $CHCl_3$ solution), (b) cells grown on patterned ITO substrate (ICR mouse 15–16 days), (c) and (d) fluorescence images of stained hippocampal neuronal cells (blue = DAPI and green = β-III tubulin). The phase-contrast micrograph and fluorescent micrographs were taken 4 days after cell seeding (5.0×10^4 cells cm^{-2}). All scale bars are 100 μm (Line width = 40 μm and spacing = 200 μm).

We have conducted immunofluorescent staining of cortical neurons using DAPI and β-tubulin as a specific antibody for clear observation. As expected, we could rarely find neuronal cells adhered to the space area. In our previous report, we were not able to completely confine neuronal cells in the grid area and some neuronal cells were frequently resident in the space area, which consisted of ITO.[15] This dramatic enhancement of cell confinement is mainly caused by the cell-repelling role of hydrophobic Br-PF. Hydrophobic Br-PF repels not only the neuronal cell body but also the neurites so that the extension of neurites crossing the space zone is completely restricted. The combination of neuronal cell adhesive m-PEI and repelling Br-PF would be effective in acquiring the single neuronal cell signal from the interface between neuronal tissue and electrode by increasing the probability of the electrode to face a single neuronal cell. Even though this approach is not limited to the combination of m-PEI and Br-PF, Br-PF is advantageous in that facile processing is possible.

We have also tried the single cell level neuronal network by reducing the line width of the grid from 40 μm to 10 μm. As can be seen in Fig. 6, a clear single cell level neuronal network was achieved with excellent pattern fidelity. This result would, when coupled with MEA, enable us to better understand the fundamental meaning of activity-dependent neuronal networks and neuron–neuron interaction as well as neuron–surface interaction. The directional control of patterned growth *via* electric field or gradient profile of adhesive molecules should reinforce the precise control of neuronal networks both at the cellular and neurite level.

Conclusions

We have synthesized photocrosslinkable Br-PF, spectroscopically analyzed the photocrosslinking process, and fabricated various patterns *via* photocrosslinking. The photocrosslinking process is facile enough that the typical photoexposure time required is a few minutes which is much shorter than the photobleaching time of 90 min for m-PEI. From the grid-space type pattern with the outmost surface of the grid and the space consisting of m-PEI and Br-PF, respectively, we could confirm the neuronal cell-repellant property of Br-PF and hence obtain excellent pattern fidelity of primarily cultured neuronal cells. We have also achieved a clear single cell level neuronal network from the grid with a line width of 10 μm. Finally, we add the biocompatible, hydrophobic, photocrosslinkable without an initiator, and fluorescent Br-PF as a member of the patternable materials useful for confining neuronal cells within a desired site, such as an electrode in MEAs.

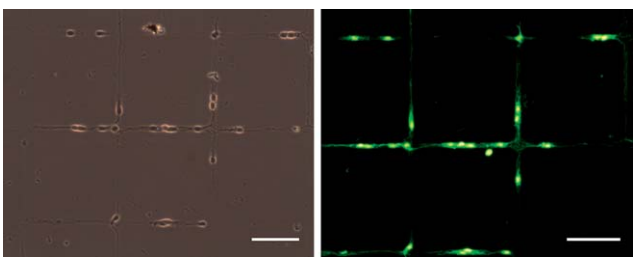

Fig. 6 A single cell level neuronal network formed on a pattern with a grid line width of 10 μm and spacing of 200 μm (1.0×10^4 cells cm^{-2}, 3 DIV). Scale bars are 100 μm.

Experimental

Materials and instruments

1,6-Dibromohexane, 2,7-dibromofluorene, tetrabutylammonium bromide (TBAB), 1-bromooctane, tetrakis(triphenylphosphine) palladium(0) ($Pd(PPh_3)_4$), 2-isopropoxy-4,4,5,5-tetramethyl-1,3,2-dioxaborolane, *n*-butyllithium (2.5 M in hexane), 20% tetrabutylammonium hydroxide (TBAH) and anhydrous toluene were purchased from Aldrich Co., and used without further purification. Tetrahydrofuran (THF) was distilled over sodium benzophenone ketyl under nitrogen prior to use. Trimethoxysilylpropyl modified poly(ethyleneimine) (M_w 1500–1800, 50% in isopropanol) was purchased from Gelest Inc. ^{1}H-NMR and ^{13}C-NMR spectra were recorded with the use of Varian Oxford 300 MHz spectrometers; chemical shifts were reported in ppm units with tetramethylsilane as an internal standard and the mass spectra were taken by a JEOL JMS-AX505WA mass spectrometer. The attenuated total reflection-Fourier transform infrared (ATR-FTIR) spectrum was taken on a Nicolet iN10 spectrometer with Ge crystal. X-ray photoelectron spectroscopy (XPS) were performed by ESCALAB 200R instrument (VG scientific) using monochromized Al-Kα operated at 1486.6 eV, 12.5 kV and 250 W X-ray radiation. The base pressure of the system was 5.0×10^{-10} Torr. XPS spectra acquired at 90° takeoff angle (TOA) relative to the surface. The molecular weight and polydispersity were analyzed by a Waters 1515 gel permeation chromatograph (GPC) with a refractive index detector at room temperature (THF as the eluent). Steady-state absorption spectra were recorded by a Shimadzu UV-2401PC spectrophotometer and photoluminescence spectra were measured by steady-state fluorimeter (Edinburgh FS920) with 450 W Xe-lamp.

2,7-dibromo-9,9′-bis(6′′-bromohexyl)fluorene (M1)[21]. To mixture of 2,7-dibromofluorene (1.0 g, 3.09 mol), 1,6-dibromohexane (6.12 g, 40.12 mol) and catalytic amounts of tetrabutylammonium bromide in DMSO, 3 mL of 50% aqueous NaOH was added. The reaction mixture was stirred for 24 h at r.t. and then poured into dilute hydrochloric acid. The aqueous layer was extracted by ethyl acetate. The combined extracts were washed with water and $NaHCO_3$ solution and then dried over $MgSO_4$. Removal of the solvent under vacuum followed by flash chromatography using hexane/dichloromethane produced a white solid (1.41 g, 70%). mp = 70–72 °C; δ_H(300MHz; $CDCl_3$; Me_4Si) 7.50 (2H, d), 7.43 (2H, d), 7.41 (2H, s), 3.28 (4H, t), 1.90 (4H, t), 1.65 (4H, m), 1.18 (4H, m), 1.06 (4H, m), 0.56 (4H, m); δ_C (75MHz; $CDCl_3$; Me_4Si) 152.1, 139.0, 130.4, 126.3, 121.6, 121.2, 55,5, 39.9, 33.6, 32.5, 28.9, 27.5, 23.4.

2,7-Dibromo-9,9-dioctyl-9*H*-fluorene[22]. To mixture of 2,7-dibromofluorene (1 g, 3.09 mol), 1-bromooctane (1.1 mL, 6.48 mol) and catalyst amounts of tetrabutylammonium bromide in 10 mL of DMSO, 3 mL of 50% aqueous NaOH was added. The reaction mixture was stirred and heated at 100 °C for 10 h and then poured into dilute hydrochloric acid. The aqueous layer was extracted by dichloromethane. The combined extracts were

washed with water and $NaHCO_3$ solution and then dried over $MgSO_4$. The mixture was purified by flash chromatography with an eluent of hexane to give a white solid (1.4 g, 83%). mp 45–47 °C (from hexane); δ_H(300MHz; $CDCl_3$; Me_4Si) 7.52 (2H, d), 7.44 (2H, d), 7.43 (2H, s), 1.90 (4H, m), 1.27–1.02 (20H, m), 0.82 (6H, t), 0.57 (4H, m); δ_C(75MHz; $CDCl_3$; Me_4Si) 152.5, 139.0, 130.2, 126.1, 121.3, 121.1, 55.5, 40.2, 31.8, 29.7, 29.1, 23.5, 22.7, 14.2.

2,2′-(9,9-dioctyl-9*H*-fluorene-2,7-diyl)bis(4,4,5,5-tetramethyl-1,3,2-dioxaborolane) (M2)[33]. *n*-Butyllithium (2.5 M in hexane; 2.4 mL, 6.0 mmol) was added slowly over 30 min to a stirred solution of 2,7-dibromo-9,9′-dioctylfluorene (1.5 g, 2.7 mmol) in dry tetrahydrofuran (70 mL) at −78 °C. The mixture was stirred for 1 h at the same temperature and then 2-isopropoxy-4,4,5,5-tetramethyl-1,3,2-dioxaborolane (1.7 mL, 8.2 mmol) was added slowly. The mixture was allowed to warm up slowly to room temperature and stirred vigorously overnight. The reaction was quenched with water and the residue was extracted with dichloromethane. The combined organic phase was dried over $MgSO_4$ and evaporated under reduced pressure. The crude product was purified by flash chromatography on silica gel and recrystallised from acetone to give the title compound as colourless crystals (1.3 g, 74%). δ_H(300MHz; $CDCl_3$; Me_4Si) 7.83 (2H, d), 7.74–7.72 (4H, m), 1.96 (4H, m), 1.42 (24H, s), 1.26–1.05 (20H, m), 0.81 (6H, t), 0.62 (4H, m); δ_C(75MHz; $CDCl_3$; Me_4Si) 150.5, 143.5, 133.3, 128.6, 119.4, 119.3, 83.7, 55.5, 40.1, 31.8, 29.8, 29.1, 29.0, 24.9, 23.7, 22.7, 14.1.

Poly[(9,9′-dioctylfluorene)-*co*-alt-(9,9′-bis(6-bromohexyl)fluorine)] (Br-PF). Compound M1 (200 mg, 0.31 mmol), compound M2 (198 mg, 0.31 mmol), and tetrakis(triphenylphosphine) palladium(0) (18 mg, 0.02 mmol) were dissolved in 10 mL of anhydrous toluene at room temperature under a nitrogen atmosphere. 3 mL of 20% Bu_4NOH were added and stirred for 30 min. The mixture was stirred vigorously at reflux for 2 days. After reaction, the mixture was poured into methanol. The crude polymeric product was filtered off and dissolved in dichloromethane. The solution was filtered through a μ-membrane filter (0.25 μm) to remove residual catalyst particles and reprecipitated in methanol. Finally the polymer was purified by Soxhlet extraction with acetone and methanol. The polymer was dried in a vacuum oven at 50 °C for 1 day, yielding 230 mg (69%) yellowish solid. GPC (THF, polystyrene standard) δ_H(300MHz; $CDCl_3$; Me_4Si) 7.85–7.62 (12H, m), 3.15 (4H, m), 2.2–2.02 (4H, m), 1.72 (4H, m), 1.26–1.05 (32H, m), 0.85 (14H, m); $M_n = 1.2 \times 10^4$ g mol^{-1}, PDI = 2.3.

Surface modification and photopatterning

Before surface modification, ITO substrates were cut into 1 cm × 1 cm and sonicated in acetone, methanol and pure water for 10 min each, followed by immersing into $NH_3 : H_2O_2 : H_2O$ mixture solution (1 : 4 : 20 v/v) at 70 °C for 1 h. After which the ITO surface was silanized with m-PEI by immersing in 2% m-PEI in anhydrous EtOH for 12 h at room temperature followed by baking at 120 °C for 10 min to reinforce covalent binding of silanol moieties. The m-PEI-coated substrate was sonicated in a bath of ethanol for 5 min for removal of non-specifically bound m-PEI. For spin coating 10 mg of photopatternable Br-PF was dissolved in 1 mL $CHCl_3$ and filtered through a 0.2 μm PTFE filter prior to spin coating. The dissolved polymer solution was spin-coated onto the m-PEI-coated ITO substrate at 1500 rpm for 30 s followed by baking at 80 °C on a hotplate for 70 s to remove solvent. Photocrosslinking was carried out using Cr mask on a mask aligner (MIDAS System Co., MDA-400M, $\lambda_{325nm} = 60$ mW cm^{-2}) as shown in Scheme 2.

Neuronal cell culture and immunofluorescent staining

A primary neuronal cell suspension was prepared from the cerebral cortex of fetal ICR mice (15–16 days of gestation) as previously described with minor modifications.[34] The cell suspension was then plated on photopatterned substrate in a 12 well culture plate at a cell density of 5×10^4. The culture medium of neurobasal medium (Invitrogen) was supplemented with a 2% B27 supplement and 1% N_2 supplement, 2.0 mM glutamine with antibiotics. To prevent the proliferation of non-neuronal cells, cytosine arabinoside (3 μM) was added to the cultures 24 h after plating. The culture medium was replaced with fresh medium without cytosine arabinoside every 3 days. The cells were cultured at 37 °C in a humidified atmosphere of 5% CO_2 and 95% air. Anti-β-tubulin (Covance, Emeryville, CA) and 4′,6-diamidino-2-phenylindole dihydrochloride (Invitrogen, Carlsbad, CA) were used for identification of neurons by immunofluorescent staining and the detailed procedure is described elsewhere.[15]

Acknowledgements

The authors greatly acknowledge the financial support from Ministry of Education, Science and Technology (Global Partnership Program, Project No. 2009-00503) and Electronics and Telecommunications Research Institute (Project No. 11ZC1130). T.-D. Kim acknowledges the Korean Research Council Industrial Science and Technology (SK-0903-01).

Notes and references

1 I. H. Lelong, V. Petegnief and G. Rebel, *J. Neurosci. Res.*, 1992, **32**, 562–568; A. I. Belenkov, V. Y. Alakhov, A. V. Kabanov, S. V. Vinogradov, L. C. Panasci, B. P. Monia and T. Y. K. Chow, *Gene Ther.*, 2004, **11**, 1665–1672.
2 B. Liu, J. Ma, E. Gao, Y. He, F. Cui and Q. Xu, *Biosens. Bioelectron.*, 2008, **23**, 1221–1228.
3 M. Maher, J. Pine, J. Wright and Y.-C. Tai, *J. Neurosci. Methods*, 1999, **87**, 45–56.
4 Q. Liu, H. Cai, Y. Xu, Y. Li, R. Li and P. Wang, *Biosens. Bioelectron.*, 2006, **22**, 318–322.
5 J. K. Chapin, *Nat. Neurosci.*, 2004, **7**, 452–455; C. T. Moritz, S. I. Perlmutter and E. E. Fetz, *Nature*, 2008, **456**, 639–642.
6 J. C. Chang, G. J. Brewer and B. C. Wheeler, *Biosens. Bioelectron.*, 2001, **16**, 527–533; J. C. Chang and G. J. Wheeler, *J. Neural Eng.*, 2006, **3**, 217–226.
7 V. S. Polikov, P. A. Tresco and W. M. Reichert, *J. Neurosci. Methods*, 2005, **148**, 1–18.
8 J. C. Chang, G. J. Brewer and B. C. Wheeler, *Biomaterials*, 2003, **24**, 2863–2870; F. Patolsky, B. P. Timko, G. Yu, Y. Fang, A. B. Greytak, G. Zhang and C. M. Lieber, *Science*, 2006, **313**, 1100–1104.
9 W. C. Chang and D. W. Sretavan, *Langmuir*, 2008, **24**, 13048–13057; K. Kang, G. Kang, B. S. Lee, I. S. Choi and Y. Nam, *Chem.–Asian J.*, 2010, **5**, 1804–1809; A. M. Leclair, S. S. G. Ferguso and F. Lagugné-Labarthet, *Biomaterials*, 2011, **32**, 1351–1360.

10 T. G. Ruardij, M. H. Goedbloed and W. L. C. Rutten, *IEEE Trans. Biomed. Eng.*, 2000, **47**, 1593–1599; H. Sorribas, C. Padeste and L. Tiefenauer, *Biomaterials*, 2002, **23**, 893–900.
11 C. S. Chen, M. Mrksich, S. Huang, G. M. Whitesides and D. E. Ingber, *Biotechnol. Prog.*, 1998, **14**, 356–363; L. Yan, W. T. S. Huck, X.-M. Zhao and G. M. Whitesides, *Langmuir*, 1999, **15**, 1208–1214; L. Lauer, C. Klein and A. Offenhäusser, *Biomaterials*, 2001, **22**, 1925–1932.
12 L. Lauer, C. Klein and A. Offenhäusser, *Biomaterials*, 2001, **22**, 1925–1932; C. G. Specht, O. A. Williams, R. B. Jackman and R. Schoepfer, *Biomaterials*, 2004, **25**, 4073–4078; H. D. Hwang, G. Kang, J. H. Yeon, Y. Nam and J.-K. Park, *Lab Chip*, 2009, **9**, 167–170.
13 B. Lom, K. E. Healy and P. E. Hockberger, *J. Neurosci. Methods*, 1993, **50**, 385–397.
14 A. Reska, P. Gasteier, P. Schulte, M. Moeller, A. Offenhäusser and J. Groll, *Adv. Mater.*, 2008, **20**, 2751–2755.
15 N. S. Baek, J.-H. Lee, Y. H. Kim, B. J. Lee, G. H. Kim, I.-K. Kim, M.-A. Chung and S.-D. Jung, *Langmuir*, 2011, **27**, 2717–2722.
16 K.-Y. Pu and B. Liu, *Biosens. Bioelectron.*, 2009, **24**, 1067–1073; X. Duan, L. Liu, F. Feng and S. Wang, *Acc. Chem. Res.*, 2010, **43**, 260–270.
17 Y. Tain, C.-Y. Chen, H.-L. Yip, W.-C. Wu, W.-C. Chen and A. K.-Y. Jen, *Macromolecules*, 2010, **43**, 282–291.
18 Q. Ji, X. Jiang and J. Yin, *Langmuir*, 2007, **23**, 12663–12668; E. Scheler and P. Strohriegl, *J. Mater. Chem.*, 2009, **19**, 3207–3212.
19 J. Y. Park, J. H. Lee and J.-B. Kim, *Eur. Polym. J.*, 2008, **44**, 3981–3986; P.-H. Wang, M.-S. Ho, S.-H. Yang, K.-B. Chen and C.-S. Hsu, *J. Polym. Sci., Part A: Polym. Chem.*, 2010, **48**, 516–524.
20 Y. Tang, L. Ji, R. S. Zhu, Z. R. Wei and B. Zhang, *J. Phys. Chem. A*, 2005, **109**, 11123–11126; K. S. Lee, K. Y. Yeon, K. H. Jung and S. K. Kim, *J. Phys. Chem. A*, 2008, **112**, 9312–9317; B. J. Kim, Y. Miyamoto, B. Ma and J. M. J. Fréecht, *Adv. Funct. Mater.*, 2009, **19**, 2273–2281.
21 X.-H. Zhou, J.-C. Yan and J. Pei, *Macromolecules*, 2004, **37**, 7078–7080; H.-H. Lu, C.-Y. Liu, T.-H. Jen, J.-L. Liao, H.-E. Tseng, C.-W. Huang, M.-C. Hung and S.-A. Chen, *Macromolecules*, 2005, **38**, 10829–10835.
22 M.-C. Hung, J.-L. Liao, S.-A. Chen, S.-H. Chen and A.-C. Su, *J. Am. Chem. Soc.*, 2005, **127**, 14576–14577.
23 C. J. Brinker and G. W. Scherer, in *Sol–Gel Science: The Physics and Chemistry of Sol–Gel Processing*, Elsevier, Oxford, UK, 1990, Ch. 2, pp. 97–228.
24 Q.-H. Xu, B. S. Gaylord, S. Wang, G. C. Bazan, D. Moses and A. J. Heeger, *Proc. Natl. Acad. Sci. USA*, 2004, **101**, 11634–11639.
25 J. Teetsov and M. A. Fox, *J. Mater. Chem.*, 1999, **9**, 2117–2122; G. Zeng, W.-L. Yu, S.-J. Chua and W. Huang, *Macromolecules*, 2002, **35**, 6907–6914.
26 G. Klaerner and R. D. Miller, *Macromolecules*, 1998, **31**, 2007–2009.
27 C.-H. Chou, S.-L. Hsu, K. Dinakaran, M.-Y. Chiu and K.-H. Wei, *Macromolecules*, 2005, **38**, 745–751; H.-H. Lu, C.-Y. Liu, T.-H. Jen, J.-L. Liao, H.-E. Tseng, C.-H. Huang, M.-C. Hung and S.-A. Chen, *Macromolecules*, 2005, **38**, 10829–10835.
28 J.-I. Lee, V. Y. Lee and R. D. Miller, *ETRI J.*, 2002, **24**, 409–414.
29 L. Romaner, A. Pogantsch, P. S. De Freitas, U. Scherf, M. Gaal, E. Zojer and E. J. W. List, *Adv. Fuct. Mater.*, 2003, **13**, 597–601.
30 V. N. Bliznyuk, S. A. Carter, J. S. Scott, G. Klärner, R. D. Miller and D. C. Miller, *Macromolecules*, 1999, **32**, 361–369; X. Gong, P. K. Iyer, D. Moses, G. C. Bazan, A. J. Heeger and S. S. Xiao, *Adv. Funct. Mater.*, 2003, **13**, 325–330.
31 M. Beinhoff, A. T. Appapillai, L. D. Underwood, J. E. Frommer and K. R. Carter, *Langmuir*, 2006, **22**, 2411–2414.
32 Y. Ofir, N. Zenou, I. Goykman and S. Yitzchaik, *J. Phys. Chem. B*, 2006, **110**, 8002–8009; M. R. Lockett and L. M. Smith, *Langmuir*, 2009, **25**, 3340–3343.
33 B. Liu and G. C. Bazan, *J. Am. Chem. Soc.*, 2006, **128**, 1188–1196; B. Liu and S. K. Dishari, *Chem.–Eur. J.*, 2008, **14**, 7366–7375.
34 X. Q. Wang and S. P. Yu, *J. Neurochem.*, 2005, **93**, 1515–1523.